RSC Advances

ROYAL SOCIETY OF CHEMISTRY

www.rsc.org/advances

Journal Name

ARTICLE

pH- and glutathione-responsive release of curcumin from mesoporous silica nanoparticles coated using tannic acid-Fe(III) complex†

Received 00th January 20xx,
Accepted 00th January 20xx

DOI: 10.1039/x0xx00000x

www.rsc.org/

Sanghoon Kim,[a,b*] Stéphanie Philippot,[a,c,d] Stéphane Fontanay,[a,c,d] Raphaël E. Duval,[a,c,d] Emmanuel Lamouroux,[a,b] Nadia Canilho,[a,b] and Andreea Pasc[a,b*]

A novel pH- and glutathione-responsive drug delivery system has been developed by deposition of tannic acid (TA) -Fe(III) complex on the surface of mesoporous silica nanoparticles (MSN). The coating was easily accomplished within 30 seconds by successive addition of iron chloride ($FeCl_3$) and tannic acid in aqueous dispersion of MSN (e.g. MCM-41). A hydrophobic model drug, curcumin, showed sustainable drug release under physiological condition (pH 7.4), while a rapid curcumin release was triggered by lowering the pH to 6.0 or 4.5. Moreover, curcumin release could be controlled by adjusting the glutathione level, which accelerate the decomposition of TA-Fe(III) complex by competitive liganding. Therefore, these results would allow developing novel and simple pH- and glutathione-responsive drug delivery systems with potential applications such as in biomedicine.

Introduction

In the past decade, mesoporous silica nanoparticles (MSN)[1] have attracted great attention as a potential drug delivery system (DDS) owing to their unique properties such as tunable pore size, large pore volume and surface area, good biocompatibility, and easy synthesis and functionalization. [2-5] In addition, mesoporous silica nanoparticles are able to load and protect a wide range of therapeutic molecules during drug delivery.[6,7] Especially, a stimuli-responsive drug delivery system is of high interest in clinical medicine to enhance therapeutic efficiency by minimizing the side effect and controlling drug release.[8] Numerous stimuli-responsive drug delivery system based on MSN have been proposed, demonstrating controllable drug release under different external or initial stimuli such as light,[9,10] pH variation,[11,12] enzyme,[13] temperature,[14] or magnetic field.[15] The main idea of designing stimuli-responsive mesoporous silica as drug delivery system relies on the surface functionalization with a gatekeeper (*i.e.* metallic nanoparticle,[16-18] organic molecules,[19,20]), targeting ligands, [21,22] or polymers[23] for mesopore sealing. In addition, organic-inorganic hybrid mesoporous silica materials have also been developed using solid lipid nanoparticles (SLN),[24,25] micelles,[26,27] with some advantages over conventional MSN, such as a high drug loading capacity. Nevertheless, the synthesis of aforementioned stimuli-responsive drug delivery systems consists in a multi-step strategy, especially during the gate-sealing step.[28,29] Therefore, it is necessary to design novel drug delivery system based on mesoporous silica with a simplified method for the industrial production. Among the synthetic strategies proposed, the surface coating[30-33] appears to be a straightforward approach because it could be easily scaled up, since the essential techniques like spray drying, have been widely adopted in pharmaceutical industry.[34]

Indeed, the development of pH- or glutathione-responsive drug delivery system has been one of the main topics for scientists, because the cancer tissues show generally more acidic environment, and their glutathione (GSH) level are also 4-fold higher than those of normal tissues.[35] Thus, the drug carrier should be stable at physiological condition (pH 7.4) without drug release to reduce the side effect on normal tissue. However, the carrier has to release the encapsulated drug when it reaches a slightly lower pH zone such as in cancer tissue (pH 5 - 6). In addition, for more efficient targeting drug delivery, it is also preferred that drug release is controlled by glutathione concentration level. For this goal, a gatekeeper approach already showed its excellent efficiency.[36,37] However, metallic nanoparticles as keepers could induce toxicity[38], which might limits their practical applications.

Very recently, an extremely rapid, one-step coating method using coordination complex of natural polyphenols, tannic acid and Fe(III) ions has been reported.[39,40] The resulting film prepared using this complex showed pH-dependent behavior,

[a] CNRS, UMR 7565, SRSMC, F-54506 Vandoeuvre-les-Nancy, France
[b] Université de Lorraine, UMR 7565, SRSMC, Faculté des Sciences et Technologies, F-54001 Vandoeuvre-les-Nancy, France
[c] Université de Lorraine, UMR 7565, SRSMC, Faculté de Pharmacie, F-54001 Nancy, France
[d] ABC Platform®, F-54001 Nancy, France
E-mail: sanghoon.kim@univ-lorraine.fr (SK), andreea.pasc@univ-lorraine.fr (AP)

† Electronic Supplementary Information (ESI) available: [SEM-EDS images, calculation of tannic acid-Fe(III), and curcumin amount in the silica materials, characterisation data of SBA-15 type materials]. See DOI: 10.1039/x0xx00000x

with a good stability above pH 7 due to multivalent coordination. Afterward, the film becomes less stable as the pH decreases, forming a bis-complex, then a mono-complex between tannic acid and Fe(III) ions. Moreover, the decomposition rate of tannic acid-Fe(III) complex could be controlled by addition of strong ligand such as EDTA.

In this framework, we designed herein a new drug delivery system using tannic acid-Fe(III) complex deposition on the outer surface of mesoporous silica nanoparticles (MSN-TA), with the aim to provide pH- and glutathione-responsive drug release, to inhibit burst release at early stages as well as to increase the bioavailability. Tannic acid-Fe(III) complex deposition was conducted by a successive addition of Fe(III) and tannic acid into the aqueous dispersion of mesoporous silica nanoparticles within 30 seconds. The resulting silica nanoparticles were characterized by various techniques, including small and wide angle X-ray scattering (SAXS and WAXS), nitrogen adsorption/desorption measurements, dynamic light scattering (DLS), diffuse reflectance UV-vis (DR UV-vis) spectroscopy, and scanning and transmission electron microscopies (SEM and TEM). To demonstrate the potential application of novel MSN-TA, *in vitro* curcumin release experiments were carried out, showing a significant suppression of drug release at pH 7.4, while a fast but sustained curcumin release was observed below pH 6. It was also shown that glutathione (GSH), which would also induce a competitive liganding with Fe(III), can trigger the curcumin release. In addition, tannic acid is generally recognized as safe (GRAS) ingredient by the U.S. Food and Drug Administration.[41] Cell viability tests were also performed and showed that the newly designed mesoporous silica nanoparticles have potential for *in vivo* applications.

Experimental

Chemicals

Tetramethylorthosilicate (TMOS), tetraethylorthosilicate (TEOS), Pluronic P123 and hexadecyltrimethylammonium bromide (CTAB), tannic acid (TA), sodium hydroxide (NaOH), glutathione (reduced form (GSH)), curcumin, sodium dodecyl sulfate (SDS) and thiazozyl blue tetrazolium bromide (MTT) were purchased from Sigma-Aldrich. Ethanol, methanol and iron (III) chloride ($FeCl_3$) was purchased from Alfa Aesar. Deionized water was purified using a Milli-Q pack system. All reagents were used as received, except phosphate buffered saline (PBS), which was sterilized before use.

Synthesis of mesoporous silica nanoparticles, MCM-41

MCM-41 was synthesized as previously reported.[42,43] Briefly, 300 mg of CTAB was dissolved in 120 g of deionized water at 35°C and kept under stirring to obtain a clear solution. Then, 0.35 mL of 2M NaOH solution was added, and the mixture was heated to 80°C. Afterward, 0.67 ml of TEOS was added as silica precursor, kept under continuous stirring for additional 2 h. The as-synthesized product was filtered and washed with deionized water then calcinated at 550°C for 5 h, giving mesoporous silica nanoparticles of MCM-41 type.

Curcumin loading into MCM-41

Curcumin loading was performed using a rotavapor as reported in the literature.[44] Briefly, 10 mg of curcumin was dissolved in 5 mL of methanol, and then 100 mg of MCM-41 was added to this solution. The mixture was sonicated for 5 min, and the solvent was slowly removed using rotary evaporator at 50 °C for 2 h. This product was kept at 30 °C for more than 24 h to remove the residual solvent. Dried curcumin loaded mesoporous silica nanoparticles are denoted as MCM-41-CU.

Coating of curcumin loaded MCM-41 using tannic Acid-Fe(III) complex

Deposition of the tannic acid-Fe(III) complex on MCM-41 was conducted by the method reported by Ejima et al.[39] with slight modifications. In brief, 0.020 mL of tannic acid solution (24 mM) and 0.020 mL of $FeCl_3$ solution (24 mM) were added to 4 mL of MCM-41-CU (1 mg/ 1 mL) under vortex stirring for 30 seconds. 0.15 mL of phosphate buffer solution (pH 8.0, 100 mM) was added to the mixture to raise the pH value around 7.2. The resulting suspension product was decanted and then the supernatant was removed. The silica materials were filtered and washed with 3 mL of deionized water for 3 times to remove any residual tannic acid-Fe(III) and phosphate salt, then dried at 35 °C for 48 h. The final products, tannic acid-Fe(III) complex coated curcumin loaded silica materials are denoted as MCM-41-CU-TA. Multi-layer coating of curcumin loaded silica materials was performed on MCM-41-CU-TA by repeating the procedure described above up to 3 times, and the product is denoted as MCM-41-CU-TA-*n*, where *n* is the number of repeated coating process. Besides, tannic acid-Fe(III) complex coated silica materials without curcumin loading were also prepared to calculate the weight percentage of tannic acid-Fe(III) complex deposited on the surface of silica materials, and the sample is denoted as MCM-41-TA.

In vitro drug release experiments

Release experiments were carried out for MCM-41-CU and MCM-41-CU-TA. The appropriate amount of material containing 1 mg of curcumin was weighted and dispersed in 75 mL of 0.3 wt% of CTAB contained dissolution medium (pH 7.4, 6.0 and 4.5) using phosphate or acetate buffer system. The ionic strength of the receiving phase was adjusted to 10 mM in the experiments at various pH values, and to 30 mM in the experiments of GSH-triggered release. The release experiments were maintained at 25°C under magnetic stirring at 100 rpm. At predetermined times, 1.5 mL aliquots were withdrawn and replaced by an equal volume of dissolution media. The withdrawn samples were centrifuged at 5000 rpm for 5 min and the supernatants were filtered on a 0.45 μm membrane filter. The released curcumin was analysed using a UV-Vis spectrometer and its concentration was calculated

using a standard curve of curcumin established for each dissolution medium. The cumulative release percentage was calculated using a dilution factor correction. All data reported are the mean value with standard deviation of at least three different experiments.

Cell line and culture conditions

MRC-5 (ATCC CCL-171) human lung fibroblasts were used as model for cytotoxic assays. Cells were grown in Minimum Essential Medium (MEM, 31095-029, Life Technologies-Gibco) supplemented with 10% heat-inactivated fetal calf serum (CVFSV00-0U, Eurobio, Courtaboeuf, France) and 2 mM L-glutamine (G7513-100ML, Sigma Aldrich), at 37°C in a 5% CO_2 humidified atmosphere.

Cytotoxicity assay on MRC5 cell line

The impact of MCM-41, MCM-41-CU, MCM-41-CU-TA, and MCM-41-TA (without curcumin) on cell viability was evaluated by the MTT assay[45] based on the reduction of MTT by mitochondrial succinate dehydrogenase into purple formazan in living cells. Cells were plated at 10^4 cells per well in 96-well tissue culture plates (83.1835, Sarstedt) and grown for 24 hours at 37 °C in a 5% CO_2 atmosphere. Then medium was discarded and replaced by fresh medium containing increasing amounts of tested silica nanoparticles (range 1 to 150 µM curcumin equivalent) previously dispersed in the medium. Three different controls were added: medium alone, cells in medium and 150 µM curcumin equivalent in medium. Each condition was repeated in eight wells. After 48 h of incubation, medium was discarded and cells were washed with PBS. Hundred microlitres of medium containing 0.5 mg/mL MTT previously prepared in PBS, were added to each well and the plates were incubated for 4 hours at 37°C. Then formazan crystals were dissolved by the addition of 100 µl of SDS (100 µg/mL) and incubation for 3 hours in 37°C. Finally absorbance was measured at 540 nm *vs* 690 nm using a 96-well plate reader (Multiskan EX, Thermo Electron Corporation). Percentages of survival and half maximal inhibitory concentration (IC_{50}) were then calculated.

General Characterization

Small and wide angle X-ray scattering (SAXS and WAXS) measurements were carried out on a SAXSess mc^2 (Anton Paar) apparatus, using a line-collimation system. This instrument is attached to an ID 3003 laboratory X-Ray generator (General Electric) equipped with a sealed X-Ray tube (PANalytical, $\lambda_{Cu,\ K\alpha}$ = 0.1542 nm) operating at 40 kV and 50 mA. A multilayer mirror and a block collimator provide a monochromatic primary beam. A translucent beam stop allows the measurement of an attenuated primary beam at q=0. Samples were sealed between two sheets of Kapton® polyimide film, before being placed inside an evacuated sample chamber, and exposed to X-Ray beam for 15 min. Scattering of X-Ray beam was recorded on an Image Plate detector, with a sample-detector distance of 261.2 mm. All the data were then corrected for the background scattering from the Kapton® and for slit-smearing effects by a desmearing procedure using the Lake method. Transmission electron microscopy (TEM) analyses were performed using Philips CM200 microscope, operated at an accelerating voltage of 200 kV. Scanning electron microscopy (SEM) analyses were performed using JEOL JCM-6000 operating at 10 kV. The samples were prepared by deposing directly silica powders onto carbon tape. N_2 adsorption-desorption isotherms were determined on a Micromeritics Tristar 3000 sorptometer at -196°C. The mesopore size distribution was calculated by the BJH (Barret, Joyner, Halenda) method applied to the adsorption branch of the isotherm. UV-Vis spectra were recorded using a UV-Vis/NIR spectrometer (Perkin Elmer Lamda 1050).

Results and discussion

Characterization of Materials

In this study, a hydrophobic model drug, curcumin was loaded into mesoporous silica nanoparticles, MCM-41 and the drug release behavior before/after surface coating using tannic acid-Fe(III) complex was investigated. Indeed, the applications of curcumin have been limited because of it low water solubility at acidic and physiological pH and its rapid hydrolysis under alkaline conditions. In addition, its poor absorption and rapid metabolism in the human body decrease the bioavailability of curcumin.[7] Therefore, to overcome these drawbacks, it is necessary to encapsulate curcumin into a drug delivery system, here into mesoporous silica nanoparticles.

First, small angle X-ray scattering (SAXS) pattern of bare MCM-41, (Fig. 1a) exhibit three well resolved peaks at 3.7, 2.1, and 1.9 nm. The ratio of these peaks is 1:$\sqrt{3}$:2, which can be attributed to the (100), (110) and (200) reflections of the hexagonal structure. The corresponding cell parameter a_0 is estimated to be 4.3 nm (Table 1), which is in accordance with results presented elsewhere.[42,44]

For curcumin loaded mesoporous silica nanoparticles, MCM-41-CU, and for tannic acid-Fe(III) coated silica, MCM-41-CU-TA, the spectra are superimposed to those of the bare materials.

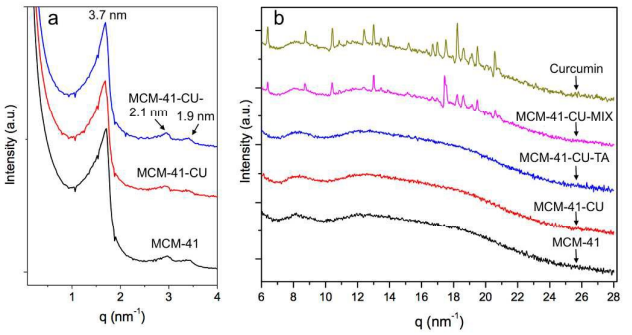

Fig. 1. a) SAXS patterns of MCM-41 with and without curcumin loading, and before and after surface coating, b) WAXS patterns of MCM-41 with and without curcumin loading, before and after surface coating, and of physical mixtures of curcumin with MCM-41.

This indicates that the hexagonal structure is maintained, and that neither the curcumin loading nor the tannic acid-Fe(III) coating seems to affect the structure of the materials.

In order to investigate the crystallinity of curcumin after encapsulation into mesopores, WAXS experiments were performed. As shown in Fig. 1b, most of characteristic peaks of pure curcumin are observed for physical mixtures of curcumin with silica nanoparticles (MCM-41-CU-MIX), suggesting that curcumin is in its crystallized form in these materials. However, for curcumin loaded mesoporous silica nanoparticles using rotavapor method (MCM-41-CU) and tannic acid-Fe(III) coated curcumin loaded mesoporous silica nanoparticles (MCM-41-CU-TA) no diffraction peak is observed in the high q-region, indicating that curcumin has been well loaded and dispersed over mesopores with an amorphous form.[44]

Nitrogen adsorption-desorption isotherm experiments were performed on bare mesoporous silica (MCM-41) and curcumin loaded mesoporous silica MCM-41-CU), showing a type IV isotherm (Fig. 2) with a capillary condensation at a relative pressure p/p_0 in the range of 0.2 - 0.4, which is characteristic of mesoporous materials. The detailed data of surface area, pore volume and pore diameter are given in Table 1. The surface area and pore volume for silica materials decrease as curcumin is loaded into mesopores, while the decrease of the pore diameter is not significant (from 2.3 nm to 2.1 nm). It is thus believed that during the evaporation of methanol at curcumin loading step, given that curcumin presents a hydrophobic nature, curcumin molecules might prefer to get together, forming nano-scale aggregates due to the presence of hydrophilic silanol groups on the surface.[44] Indeed, the rotavapor drug loading method has been widely employed for hydrophobic molecules because of its simple procedure and high drug loading efficiency that could reach around 100 %. Moreover, by this method, the drug exhibits very low ratio of crystalline phase that cannot be obtained by other methods like the fluid bed, in which the fast solvent evaporation could induce the crystallization of hydrophobic drug molecules.[46]

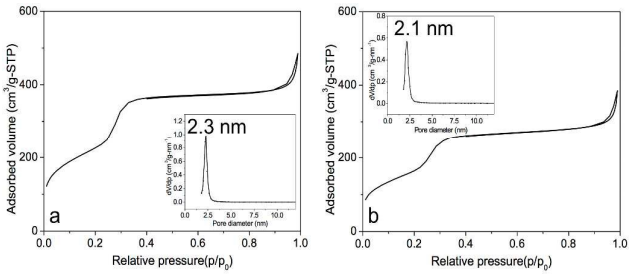

Fig. 2. N_2 adsorption–desorption isotherms and pore size distribution (inset) of (a) MCM-41, (b) MCM-41-CU

Table 1. Physicochemical properties of silica materials (MCM-41) with and without curcumin loading[a]

Sample	D_P (nm)	S_{BET} ($m^2 g^{-1}$)	V_P ($cm^3 g^{-1}$)
MCM-41	2.3	838	0.52
MCM-41-CU	2.1	640	0.40

a. D_P = Pore diameter, S_{BET} = BET surface area, V_P = Pore volume

The surface coating was then performed by adding tannic acid and Fe(III) ions in the aqueous dispersion of mesoporous silica nanoparticles. The general mechanism of one-step assembly of TA-Fe(III) could be explained, as previously reported,[39,47] by the adsorption of free TA or small TA-Fe complexes onto the surface of the substrate, here mesoporous silica nanoparticles through multiple hydrogen bonding or coordination between Fe and silanol from the silica surface.[48]

The amount of tannic acid-Fe(III) complex deposited on MSN was also calculated, (see SI for detailed calculation) giving that approximately 0.102 mg of tannic acid and 0.001 mg of Fe ions were deposited on the surface of silica nanoparticles. Thus, the weight percent of tannic acid and Fe ions is 2.5 % and less than 0.1 %, respectively.

The size measurement was performed using dynamic light scattering (DLS) for MCM-41 before/after tannic acid-Fe(III) complex coating. (Fig. 3a) The hydrodynamic mean diameter of silica nanoparticles is 217 nm for MCM-41, after curcumin loading, and then tannic acid-Fe(III) complex coating, its mean size changed to 225 nm, and 234 nm, respectively. Then, by multiple deposition of tannic acid-Fe(III) complex, the mean size increased to 248 nm, and 265 nm for 2 times (MCM-41-CU-TA-2), and 3 times (MCM-41-CU-TA-3) coated silica nanoparticles, respectively. The formation of multilayer of tannic acid-Fe(III) complex was confirmed by FT-IR measurement, showing the continuous increase of OH stretching band and C=O stretching band of tannic acid. (Fig. S1) The presence of tannic acid-Fe(III) complex in silica materials was also confirmed by the evolution of UV-Vis diffuse reflectance spectra. (Fig. 3b) For clarity reasons, only silica materials without curcumin (MCM-41-TA) were analyzed. First, no significant peak was observed for MCM-41, indicating the absence of any molecule that absorb above 300 nm. However, one peak of MCM-41-TA was observed at 307 nm, which corresponds to the tannic acid absorption peak coordinated to the Fe(III) ions, and a broad shoulder around 550 nm could be assigned to charge transfer band from a coordinated tannic acid to Fe(III) ions of tannic acid-Fe(III) tris-complex compound.[47,48]

Scanning electron microscopy (SEM) analysis was then conducted to investigate the morphologies and the surface properties of tannic acid-Fe(III) complex coated mesoporous silica nanoparticles (Fig. S2). Silica materials before/after coating showed a spherical or ellipsoid morphology with a particle size of ~ 150 nm that is in good agreement with the results obtained by DLS measurements. Since the morphology of MCM-41 silica material after tannic acid-Fe(III) coating (MCM-41-CU-TA) remained identical to its starting material (MCM-41), SEM-EDS mapping experiment was performed on MCM-41-CU-TA, showing that Fe atoms were homogenously dispersed over silica material (Fig. S3). By spotting on several areas using SEM-EDS beam, it was founded that iron content on the surface of silica materials is ~ 0.2 %, (Fig. S4, Table S1),

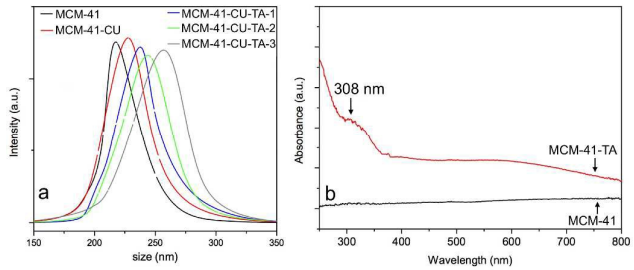

Fig. 3. (a) Size distribution of MCM-41 type silica materials obtained from DLS, (b) UV-vis spectra of MCM-41 and MCM-41-TA. For clarity reasons, UV-vis measurements were performed on the silica materials without curcumin.

which is higher than the calculated values using UV-Vis (less than 0.1 wt.%), but seems reasonable, since SEM-EDS analysis can measure only the silica surface.

Further evidence for tannic acid-Fe(III) coating on the surface of silica nanoparticles is provided by the transmission electron microscopy (TEM) images presented in Fig. 4. First, the image for bare MCM-41 (Fig. 4a) showed the typical well-ordered hexagonal pore network in spherical or ellipsoid form with the mean diameter of 155 nm with standard deviation of 27 nm, by more than counting 20 particles. The presence of tannic acid-Fe(III) complex on the surface of MSN could be visualized after coating (Fig. 4b). Especially, a zoomed image of silica nanoparticles coated 3 times (Fig. 4c, additional image in SI (Fig. S6a)) clearly showed the presence of tannic acid-Fe(III) complex coating on the surface of silica, giving the average thickness of 16.1 nm with 4.6 nm as standard deviation, by analyzing 20 particles. From this result, it is assumed that the average thickness of 1 layer of coating could be of 5.3 nm. The stability of coating as a function of pH was also monitored using TEM analysis. The samples were prepared by incubating mesoporous silica coated 3 times (MCM-41-CU-TA-3) in the buffer solutions of pH 4.5 and pH 2.5 for 1 h with 15 min of sonication. For the sample incubated at pH 4.5, (Fig. 4d) it was found that most of tannic acid-Fe(III) complex were removed, and at pH 2.5, even opened mesopores were observed. (Fig. S6b) This unique pH-dependent property of tannic acid-Fe(III) complex will further be discussed in *in vitro* curcumin release experiments section.

In vitro release experiments

The release experiments of curcumin loaded mesoporous silica nanoparticles (MCM-41-CU) and tannic acid-Fe(III) coated curcumin loaded mesoporous silica nanoparticles (MCM-41-CU-TA) were carried out in 3 different receiving solution (pH 7.4, 6.0 and 4.5) containing 0.3 wt.% of CTAB in order to

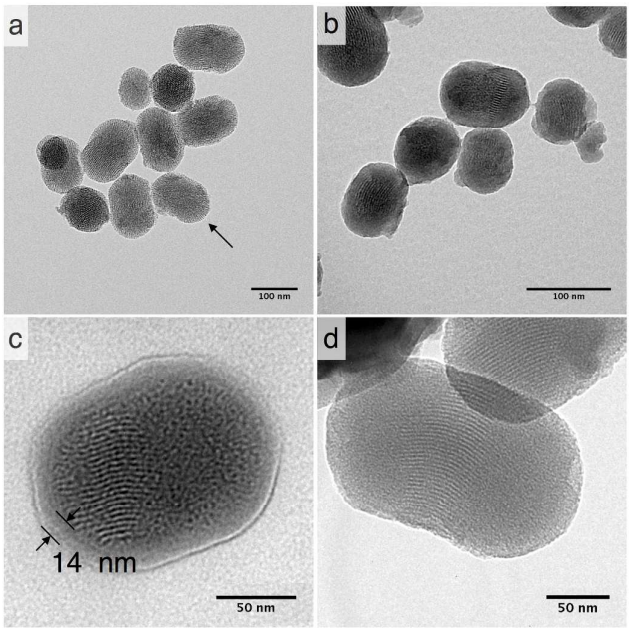

Fig. 4. TEM image of (a) MCM-41 (arrow indicates opened pores), (b) MCM-41-CU-TA, (c) MCM-41-CU-TA-3 (coated 3 times), (d) MCM-41-CU-TA-3 incubated at pH 4.5

solubilize the released curcumin[49] that is poorly soluble and rapidly degraded in water.[50]

During the release experiments, the sink condition was kept by adding the same volume of receiving solution as the withdrawn volume. As shown in Fig. 5, the curcumin release from tannic acid-Fe(III) coated MCM-41 is significantly decreased compared to non coated MCM-41, and the release profile depends on the pH values. Indeed, at pH values lower than 2, only the mono-complex TA-CU can be formed, while at pH values higher than 7, three moieties of tannic acid are strongly bonded to Fe(III).[39] (Fig. 8) The release of curcumin from MCM-41-CU-TA is effectively retained at pH 7.4, however, it is not completely suppressed, probably due to a good permeability of tannic acid-Fe(III) complex to small molecules like curcumin.[47] Since the curcumin release from tannic acid-Fe(III) coated mesoporous silica nanoparticles showed only tannic acid-Fe(III) coating dependence, the further investigations were conducted by varying some parameters concerning tannic acid-Fe(III) agent complex.

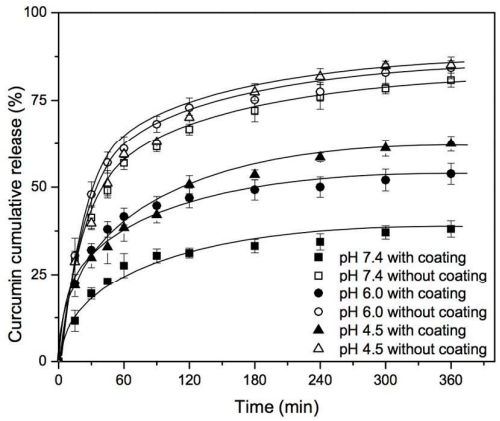

Fig. 5. Cumulative release of curcumin for MCM-41-CU, and MCM-41-CU-TA

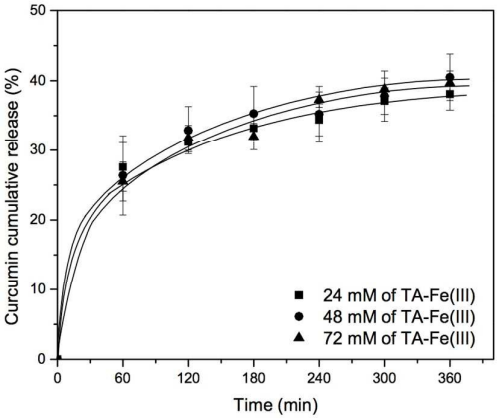

Fig. 6. Effect of coating agent concentration on curcumin release

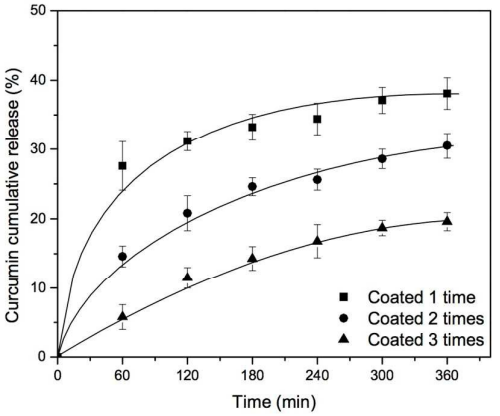

Fig. 7. Effect of multiple coating process on curcumin release

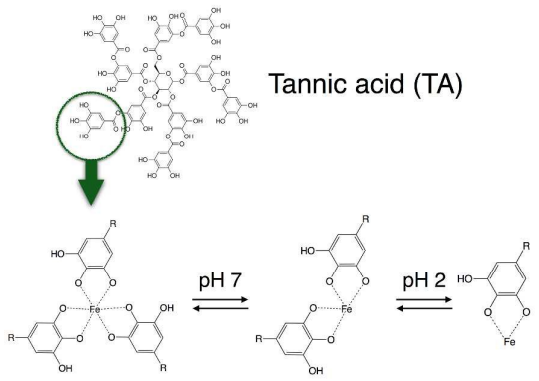

Fig. 8. Dominate complex form of tannic acid-Fe(III) as a function of pH

First, the concentration of tannic acid-Fe(III) complex was varied from 24 mM to 72 mM in order to investigate the effect of coating agent concentration on curcumin release. As shown in Fig. 6, there is no significant improvement of curcumin release at pH 7.4, even with silica material prepared using 72 mM of tannic acid-Fe(III) (MCM-41-CU-TA-72), giving about 40 % of curcumin cumulative release after 360 min, which is similar to the result of the silica material prepared with 24 mM of tannic acid-Fe(III) complex. (MCM-41-CU-TA) However, this is in a good agreement with the studies reported by Ejima et al.,[39] showing that the thickness of the complex film is not depending on the tannic acid-Fe(III) concentration. Therefore, it can be concluded that 24 mM as concentration of tannic acid-Fe(III) seems to be enough to cover all the surface of mesoporous silica nanoparticles during coating process. Afterward, the effect of multiple coating on curcumin release was also investigated. (Fig. 7) Indeed, more tannic acid-Fe(III) coating process is repeated, more curcumin release from the silica nanoparticles is effectively retained. For example, curcumin loaded MCM-41 coated 3 times with the complex (MCM-41-CU-TA-3) showed only 17 % of curcumin release after 360 min, while 38 %, and 28 % of curcumin release was obtained for MCM-41-CU-TA (coated 1 time), and MCM-41-CU-TA-2 (coated 2 times), respectively. Thus, contrary to the curcumin release result obtained by the variation of tannic acid-Fe(III) concentration, the multiple coating process seems more efficient to tailor the drug release profile, which should be due to increased thickness of tannic acid-Fe(III) complex as already discussed in TEM analysis section.

To further investigate a correlation between surface properties of silica materials and curcumin rate release, the evolution of the zeta potential of mesoporous silica nanoparticles was monitored as a function of pH. (Fig. 9) First, after tannic acid-Fe(III) coating, the zeta potential slight decreased by ~ 5 mV at pH 7.4 (cf. MCM-41-CU *vs* MCM-41-CU-TA or MCM-41 *vs* MCM-41-TA) due to the increase of the negative charge by non-coordinated galloyl groups of tannic acid.[47] Then, in all case the zeta potential values increase as pH value decreases from 7.4 to 4.0, because of the protonation of silanol groups of the silica surface. However, the increase of zeta potential is not dramatic for tannic acid-Fe(III) coated silica materials

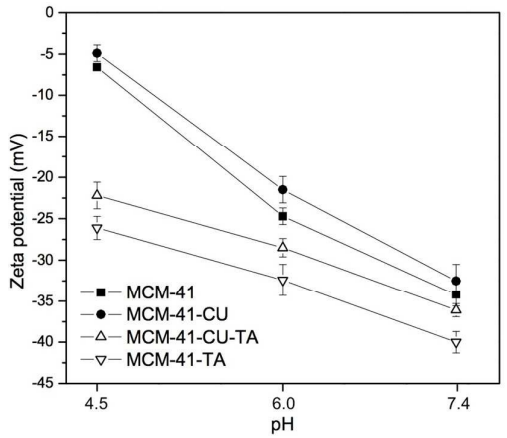

Fig. 9. Zeta potential of MCM-41 silica materials as a function of pH.

(MCM-41-CU-TA, MCM-41-TA) because in the pH range between 6.0 and 4.5, tannic acid-Fe(III) still exists as the bis-complex on the silica surface, which could shield silanol groups from the solvent. As a result, the surface silanol groups for coated silica materials are less exposed to the dissolution medium, compared to non-coated silica materials, thus the curcumin release could be also retained. Besides, the zeta potential reached around 0 mV at pH 2.5 (data not shown in Fig. 9) for all silica materials with the recovery of its original white color for MCM-41-TA (without curcumin), which indicates the total decomposition of tannic acid-Fe(III) complex as confirmed by TEM analysis.

Finally, the curcumin release in the presence of other ligand was investigated using glutathione (GSH), which has been considered as one of the most efficient internal triggers because its concentration is quite different between the exterior (2 µM) and interior (10 mM) of the cells,[51,52] and in some cancer tissues the concentration of GSH could be 4-fold higher than normal tissues. Moreover, since the thiol group of GSH can generally reduces disulfide bond linker, the main approach using GSH trigger is redox-responsive mesopores gatekeeper. However, in this study GSH that contains carboxylate group along with amine group, was used only as a metal chelator that can compete with tannic acid for iron complexation. Indeed, it was already reported that contrary to cysteine, GSH cannot reduce Fe(III) ions because of the liganding that occurs between carboxylate group of GSH and iron complex compound.[53] Indeed, glutathione is already known as a good ligand for Fe(III) ions.[54] As shown in Fig. 10, the curcumin release from MCM-41-CU-TA was slightly increased after adding GSH in dissolution medium of pH 7.4, and the rate of curcumin release could be also controlled by adjusting GSH level from 0 mM to 1.0 mM, which reaches 48 % of curcumin release at 360 min. This could be explained by dual effect: 1) a competitive liganding of GSH with tannic acid and 2) slight decrease of pH from 7.4 to 7 by adding GSH. Indeed, the stability constant (logK) of the tannic acid-Fe(III) complex varies with the pH and is of about 9 at pH 5-7 and increases drastically at pH 8 (logK=17).[55] For GSH-Fe(III) complex, its stability constant (logK) is 11 at pH 7.[54] Thus, at this pH, GSH can effectively compete with tannic acid for the formation of Fe(III)-complex.

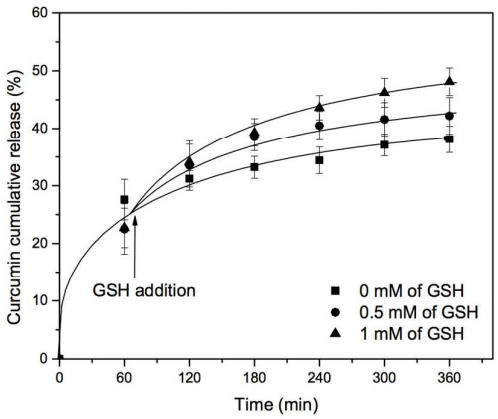

Fig. 10. Effect of glutathione (GSH) concentration level on curcumin release

In addition to MCM-41 silica nanoparticles, the feasibility of tannic acid-Fe(III) coating for large pore system was investigated using curcumin loaded SBA-15 silica materials.

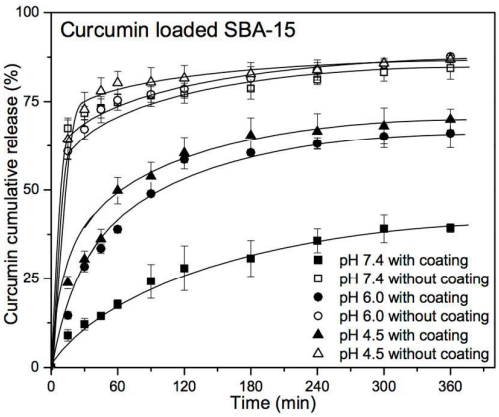

Fig. 11. Cumulative release of curcumin from SBA-15-CU, and SBA-15-CU-TA

Despite of interesting pore size of ~ 7.0 nm, (Fig. S7, S8) the morphology of SBA-15 is not well defined, showing randomly ordered block silica with more than 1 μm in diameter, as observed by SEM and TEM. (Fig. S9, S10) Moreover, due to its not-well defined morphology that might cause the bad water-dispersability, only agglomerated silica materials could be obtained after tannic acid-Fe(III) coating process. (Fig. S10b)

However, curcumin release from tannic acid-Fe(III) coated SBA-15 silica material (SBA-15-CU-TA) showed also pH-dependent release pattern, (Fig. 8) while a burst release phenomenon for non-coated SBA-15 (SBA-15-CU) was observed, due to the large pores that provide high diffusion rate. Interestingly, cumulative release values (%) after 360 min are very close to those of coated MCM-41 silica nanoparticles, which suggest that the decomposition process of tannic acid-Fe(III) complex is the crucial factor for the release of encapsulated molecules. As a result of curcumin release experiments, one can suggest that tannic acid-Fe(III) complex

coating is a powerful method for controlling the release of encapsulated molecule, especially for bulky molecules in large pore system. Work is underway for the fine deposition of tannic acid-Fe(III) on spherical silica materials with larger pore,[56] with potential applications in pharmaceutics for a controlled release of macromolecules, *i.e*. enzymes.

Cytotoxicity test

The impact of tannic acid coating of mesoporous silica nanoparticles on cell viability was tested with MRC5 cells (Table 2). After 48 hours treatment MCM-41 and MCM-41-TA showed no cytotoxicity, meaning that addition of tannic acid-Fe(III) complex on mesoporous silica nanoparticles has no impact on cell viability. However, MCM-41-CU and MCM-41-CU-TA induced higher cytotoxicity compared to curcumin alone, which is also in good agreement with previous reported results.[7] As a result, mesoporous silica nanoparticles (MCM-41) coated with tannic acid-Fe(III) would have potential biomedical applications, due to their biocompatibility and bioinertness.

Table 2. Half maximal inhibitory concentration (IC_{50}) of curcumin, MCM-41, MCM-41-CU, MCM-41-CU-TA and MCM-41-TA for the treatment of MRC5 cells (n=2)

	Curcumin	MCM-41[a]	MCM-41-CU	MCM-41-CU-TA	MCM-41-TA[a]
IC_{50} (μM)	> 150	> 150	22.1±3.8	20.2±3.5	> 150

a. IC_{50} were calculated with respect to the same amount of silica as other materials

Conclusions

It has been shown that pH-responsive curcumin-loaded mesoporous silica nanoparticles (MSN) were successfully prepared by deposition of tannic acid-Fe(III) complex on the surface of silica. Curcumin, a hydrophobic drug, was encapsulated into mesopores using simple rotary evaporation method, which prevent its crystallization inside pores. The deposition of tannic acid-Fe(III) complex on MSN resulted in multi-responsive drug delivery carrier, which triggers curcumin release upon the variation of pH or glutathione concentration level. Moreover, it was also demonstrated that the sustainability of drug release increased with the number of deposition layers of tannic acid-Fe(III) complex.

Therefore, using tannic acid-Fe(III) complex coating method is a straightforward way to design pH- and glutathione-responsive drug carrier with mesoporous silica materials, showing reduced burst release, improved stability, bioavailability and bioinertness. This strategy could provide a general route for designing various systems, combining other stimuli-responsive nanocarriers[57] or sensors.[58] Moreover, due to good biocompatibility of tannic acid,[59] this method would be also useful in various applications such as designing drug delivery systems for *in vivo* biological experiments.[60]

Acknowledgements

The authors would like to thank Grégoire Herzog and Sijin Li for SEM analysis. The authors acknowledge LCPME for SEM facilities and Mélanie Emo for performing SAXS/WAXS measurements. The French Ministry of Higher Education (MRES), the French National Scientific Center (CNRS) and Region Lorraine provided financial support. SK acknowledges the French Ministry of Higher Education (MRES) for the PhD grant.

Notes and references

1 C. T. Kresge and W. J. Roth, *Chem. Soc. Rev.*, 2013, **42**, 3663-3670.
2 V. Mamaeva, C. Sahlgren, and M. Lindén, *Adv. Drug Delivery Rev.*, 2013, **65**, 689–702.
3 P. Yang, S. Gai, and J. Lin, *Chem. Soc. Rev.*, 2012, **41**, 3679-3698.
4 C. Argyo, V. Weiss, C. Bräuchle, and T. Bein, *Chem. Mater.*, 2014, **26**, 435–451.
5 M. Vallet-Regí, F. Balas, and D. Arcos, *Angew. Chem. Int. Ed.*, 2007, **46**, 7548–7558.
6 C. Lei, Y. Shin, J. Liu, and E. J. Ackerman, *Nano Lett.*, 2007, **7**, 1050–1053.
7 S. Jambhrunkar, S. Karmakar, A. Popat, M. Yu, and C. Yu, *Rsc Advances*, 2014, **4**, 709-712.
8 S. Mura, J. Nicolas, and P. Couvreur, *Nat Mater*, 2013, **12**, 991–1003.
9 E. Aznar, M. D. Marcos, R. Martínez-Máñez, F. Sancenón, J. Soto, P. Amorós, and C. Guillem, *J. Am. Chem. Soc.*, 2009, **131**, 6833–6843.
10 D. He, X. He, K. Wang, J. Cao, and Y. Zhao, *Langmuir*, 2012, **28**, 4003–4008.
11 H. Zheng, Y. Wang, and S. Che, *J. Phys. Chem. C*, 2011, **115**, 16803–16813.
12 C. Park, K. Oh, S. C. Lee, and C. Kim, *Angew. Chem. Int. Ed.*, 2007, **46**, 1455–1457.
13 Y. Xiao, T. Wang, Y. Cao, X. Wang, Y. Zhang, Y. Liu, and Q. Huo, *Dalton Trans.*, 2015, **44**, 4355–4361.
14 Y. Jiao, Y. Sun, B. Chang, D. Lu, and W. Yang, *Chem. Eur. J.*, 2013, **19**, 15410–15420.
15 Q. Gan, X. Lu, Y. Yuan, J. Qian, H. Zhou, X. Lu, J. Shi, and C. Liu, *Biomaterials*, 2011, **32**, 1932–1942.
16 C.-Y. Lai, B. G. Trewyn, D. M. Jeftinija, K. Jeftinija, S. Xu, S. Jeftinija, and V. S. Y. Lin, *J. Am. Chem. Soc.*, 2003, **125**, 4451–4459.
17 S. Giri, B. G. Trewyn, M. P. Stellmaker, and V. S. Y. Lin, *Angew. Chem. Int. Ed.*, 2005, **44**, 5038–5044.
18 F. Muhammad, M. Guo, W. Qi, F. Sun, A. Wang, Y. Guo, and G. Zhu, *J. Am. Chem. Soc.*, 2011, **133**, 8778–8781.
19 V. Cauda, C. Argyo, and T. Bein, *J. Mater. Chem.*, 2010, **20**, 8693-8699.
20 Y. L. Choi, J. H. Lee, J. Jaworski, and J. H. Jung, *J. Mater. Chem.*, 2012, **22**, 9455-9457.
21 V. Mamaeva, J. M. Rosenholm, L. T. Bate-Eya, L. Bergman, E. Peuhu, A. Duchanoy, L. E. Fortelius, S. Landor, D. M. Toivola, M. Lindén, and C. Sahlgren, *Mol. Ther.*, 2009, **19**, 1538–1546.
22 L. Palanikumar, E. S. Choi, J. Y. Cheon, S. H. Joo, and J.-H. Ryu, *Adv. Funct. Mater.*, 2014, **25**, 957–965.
23 N. Singh, A. Karambelkar, L. Gu, K. Lin, J. S. Miller, C. S. Chen, M. J. Sailor, and S. N. Bhatia, *J. Am. Chem. Soc.*, 2011, **133**, 19582–19585.
24 R. Ravetti-Duran, J.-L. Blin, M.-J. Stébé, C. Castel, and A. Pasc, *J. Mater. Chem.*, 2012, **22**, 21540-21548.
25 S. Kim, M.-J. Stébé, J.-L. Blin, and A. Pasc, *J. Mater. Chem. B*, 2014, **2**, 7910–7917.

26 N. W. Clifford, K. S. Iyer, and C. L. Raston, *J. Mater. Chem.*, 2008, **18**, 162–165.
27 P. Botella, A. Corma, and M. Quesada, *J. Mater. Chem.*, 2012, **22**, 6394-6401.
28 Y. Zhang, Z. Zhi, T. Jiang, J. Zhang, Z. Wang, and S. Wang, *J. Controlled Release*, 2010, **145**, 257–263.
29 X. Kang, Z. Cheng, D. Yang, P. Ma, M. Shang, C. Peng, Y. Dai, and J. Lin, *Adv. Funct. Mater.*, 2012, **22**, 1470–1481.
30 S. R. Choi, D.-J. Jang, S. Kim, S. An, J. Lee, E. Oh, and J. Kim, *J. Mater. Chem. B*, 2014, **2**, 616–619.
31 W. Feng, X. Zhou, C. He, K. Qiu, W. Nie, L. Chen, H. Wang, X. Mo, and Y. Zhang, *J. Mater. Chem. B*, 2013, **1**, 5886.
32 Y. Zhu, J. Shi, W. Shen, X. Dong, J. Feng, M. Ruan, and Y. Li, *Angew. Chem. Int. Ed.*, 2005, **44**, 5083–5087.
33 Y. Zhu and J. Shi, *Microporous Mesoporous Mater.*, 2007, **103**, 243–249.
34 J. Broadhead, S. K. Edmond Rouan, and C. T. Rhodes, *Drug Dev. Ind. Pharm.*, 1992, **18**, 1169–1206.
35 K. Engin, D. B. Leeper, J. R. Cater, A. J. Thistlethwaite, L. Tupchong, and J. D. McFarlane, *Int. J. Hyperthermia*, 1995, **11**, 211–216.
36 R. Liu, Y. Zhang, X. Zhao, A. Agarwal, L. J. Mueller, and P. Feng, *J. Am. Chem. Soc.*, 2010, **132**, 1500–1501.
37 J. E. Lee, D. J. Lee, N. Lee, B. H. Kim, S. H. Choi, and T. Hyeon, *J. Mater. Chem.*, 2011, **21**, 16869-16872.
38 A. M. Schrand, M. F. Rahman, S. M. Hussain, J. J. Schlager, D. A. Smith, and A. F. Syed, *Wiley Interdiscip. Rev.: Nanomed. Nanobiotechnol.*, 2010, **2**, 544–568.
39 H. Ejima, J. J. Richardson, K. Liang, J. P. Best, M. P. van Koeverden, G. K. Such, J. Cui, and F. Caruso, *Science*, 2013, **341**, 154–157.
40 J. Guo, Y. Ping, H. Ejima, K. Alt, M. Meissner, J. J. Richardson, Y. Yan, K. Peter, D. von Elverfeldt, C. E. Hagemeyer, and F. Caruso, *Angew. Chem. Int. Ed.*, 2014, **53**, 5546–5551.
41 http://www.fda.gov/Food/IngredientsPackagingLabeling/GRAS/SCOGS/ucm2006852.htm.
42 Q. Cai, Z.-S. Luo, W.-Q. Pang, Y.-W. Fan, X.-H. Chen, and F.-Z. Cui, *Chem. Mater.*, 2001, **13**, 258–263.
43 Q.-L. Li, Y. Sun, Y.-L. Sun, J. Wen, Y. Zhou, Q.-M. Bing, L. D. Isaacs, Y. Jin, H. Gao, Y.-W. Yang, *Chem. Mater.*, 2014, **26**, 6418–6431.
44 S. Jambhrunkar, Z. Qu, A. Popat, J. Yang, O. Noonan, L. Acauan, Y. Ahmad Nor, C. Yu, and S. Karmakar, *Mol. Pharmaceutics*, 2014, **11**, 3642–3655.
45 T. Mosmann, *J. Immunol. Methods*, 1983, **65**, 55–63.
46 T. Limnell, H. A. Santos, E. Mäkilä, T. Heikkilä, J. alonen, D. Y. Murzin, N. Kumar, T. Laaksonen, L. Peltonen, and J. Hirvonen, *J. Pharm. Sci.*, 2011, **100**, 3294–3306.
47 M. A. Rahim, H. Ejima, K. L. Cho, K. Kempe, M. Müllner, J. P. Best, and F. Caruso, *Chem. Mater.*, 2014, **26**, 1645–1653.
48 H. Ozawa and M.-A. Haga, *Phys. Chem. Chem. Phys.*, 2015, **17**, 8609–8613.
49 D. Ke, X. Wang, Q. Yang, Y. Niu, S. Chai, Z. Chen, X. An, and W. Shen, *Langmuir*, 2011, **27**, 14112–14117.
50 Z. Wang, M. H. M. Leung, T. W. Kee, and D. S. English, *Langmuir*, 2010, **26**, 5520–5526.
51 A. N. Koo, H. J. Lee, S. E. Kim, J. H. Chang, C. Park, C. Kim, J. H. Park, and S. C. Lee, *Chem. Commun.*, 2008, 6570.
52 Y. Cui, H. Dong, X. Cai, D. Wang, and Y. Li, *ACS Appl. Mater. Interfaces*, 2012, **4**, 3177–3183.
53 N. Spear and S. D. Aust, *Arch. Biochem. Biophys.*, 1994, **312**, 198–202.
54 G. Berthon, *Pure & Appl. Chem*., 1995, **67**, 1117–1240.
55 S. Sungur, A. Uzar, *Spectrochim. Acta Part A*, 2008, **69**, 225–229.
56 N. Canilho, A. Pasc, M. Emo, M.-J. Stébé, and J.-L. Blin, *Soft Matter*, 2013, **9**, 10832-10840.
57 D. Hua, J. Jiang, L. Kuang, J. Jiang, W. Zheng, and H. Liang, *Macromolecules*, 2011, **44**, 1298–1302.
58 L. V. Sigolaeva, S. Y. Gladyr, A. P. H. Gelissen, O. Mergel, D. V. Pergushov, I. N. Kurochkin, F. A. Plamper, and W. Richtering, *Biomacromolecules*, 2014, **15**, 3735–3745.
59 X. Zhang, M. Liu, X. Zhang, F. Deng, C. Zhou, J. Hui, W. Liu, and Y. Wei, *Toxicol. Res.*, 2015, **4**, 160–168.
60 X. Chen, X. Cheng, A. H. Soeriyadi, S. M. Sagnella, X. Lu, J. A. Scott, S. B. Lowe, M. Kavallaris, and J. J. Gooding, *Biomater. Sci.*, 2014, **2**, 121–130.